Investigation of flexural-torsional buckling behavior of cold-formed structural channel columns

Vu Quoc Anh, Pham Ngoc Hieu

Abstract

The paper investigates both the theory and experimental behavior of thin-walled columns under flexural-torsional buckling modes. The global buckling of these such columns can be categorized into flexural, torsional, and combined flexural-torsional modes, noting that torsional and combined flexural-torsional modes are less explored and more challenging to control in experiments compared to the pure flexural buckling mode. The paper aims to determine the elastic flexural-torsional buckling load theoretically and to set up experiments to observe and analyze the column's behavior under flexural-torsional buckling. The theoretical predictions are subsequently compared with experimental results to discuss and to thoroughly understand this flexural-torsional buckling mode.

Key words: Investigation; Flexural-torsional buckling; Cold-formed structural; Channel columns

Assoc. Prof.Dr. Vu Quoc Anh
Assoc. Prof.Dr. Pham Ngoc Hieu
Faculty of Civil Engineering, Hanoi Architectural University
Mail: anhvq@hau.edu.vn; Tel: 0904715062

Date of receipt: 8/4/2024
Editing date: 22/5/2024
Post approval date: 04/11/2024

1. Introduction

Cold-formed structures have been developed for steel and aluminum materials and have been widely applied in practice. The channel section profile has been the most commonly used type worldwide for many decades due to its advantages in manufacturing, transportation, and construction [1]. In terms of overall column instability, the channel sections, as an open section, can occur buckling due to flexure, and can also experience instability due to torsion or combined flexure and torsion.

In terms of stability, the overall theoretical stability of this column type was essentially determined by the Euler formula used for the flexural buckling[2, 3]. Additionally, torsional buckling is also considered through the development of theories[2, 4-6]. Regarding practical, experiments on flexural buckling have been considered in many test programs of [7, 8], while experiments on flexural torsional buckling of columns are more difficult to conduct and require careful experimental setup to be able to control such programs accurately. One of the most recent experimental programs of flexural torsional buckling of cold-formed columns was conducted at the University of Sydney, Australia. This was a part of the project funded by the Australian Government with Project Number LP140100863, carried out in collaboration between The University of Sydney and BlueScope Permalite. The obtained results provided an understanding of the flexural torsional buckling behavior and could serve as a basis for the development of future simulation models.

The paper aims to discuss the theoretical aspects of determining the buckling instability load of cold-formed column components, focusing specifically on applying this concept to ascertain the instability load for a cold-formed channel column. Following this, the paper summarizes and analyzes the experimental setup and behavior of a cold-formed aluminum column during buckling instability. Furthermore, comparisons between theoretical predictions and experimental findings will be made to gain an understanding of how cold-formed column behaves both during and after buckling instability.

2. The theory in determining the buckling load of cold-formed structural columns

Columns with closed cross-sections often do not undergo torsional instability due to their significant resistance to torsion. For open cross-section columns, however, it is important to consider three types of global buckling modes, including flexural buckling, torsional buckling, or combined flexural-torsional buckling. The theoretical investigation into torsional and flexural-torsional bucking modes has been extensively studied by various authors such as Timoshenko, Gere [2], Trahair[4]; Winter, Chajes, and Fang [5, 6].

Figure 1 depicts a section with displacements u and v along the x and y axes, and a rotation angle Φ relative to the centroid. Considering a column in an equilibrium state under an axial compressive load P, results in various formulas:

$$EI_y u^{iv} + Pu'' + Py_o\Phi'' = 0 \quad (1)$$

$$EI_y u^{iv} + Pu'' + Py_o\Phi'' = 0 \quad (2)$$

$$EC_W\Phi^{iv} - (GJ - Pr_o^2)\Phi'' + Py_o u'' - Px_o v'' = 0 \quad (3)$$

$$r_o = \sqrt{r_x^2 + r_y^2 + x_o^2 + y_o^2}$$

where:

I_x, I_y– Second moments of areas corresponding to the x, y axes;

u, v - Displacements along the x, y axes correspondingly;

Φ –Rotation angle;

x_o, y_o–shear centre coordinates;

J - St Venant torsional constant;

C_w - the warping constant;

r_o - polar radius of gyration of the cross-section about the shear centre;

r_x, r_y - radii of gyration of the cross-section about the x- and y-axes, respectively.

The derivatives of formulas (1), (2), and (3) are taken with respect to the variable z along the component's axis. Boundary conditions are analyzed for a component with two pin ends. For z values of 0 and L, the deformations at two ends include:

$$u = v = \Phi = 0;\ u'' = v'' = \Phi'' = 0$$

Formulas (1) and (3) can be transformed into the following formula (4):

$$r_o^2(P_{cre} - P_x)(P_{cre} - P_y)(P_{cre} - P_z) - (P_{cre})^2(y_o)^2(P_{cre} - P_x) - (P_{cre})^2(x_o)^2(P_{cre} - P_y) = 0 \quad (4)$$

where buckling loads according to the x, y and z axes are determined as follows:

$$P_x = \frac{\pi^2 EI_x}{(K_x L_x)^2} \quad (5)$$

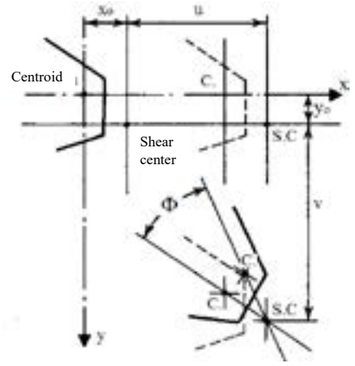

Figure 1. The deformations of sections during flexural-torsional buckling [6]

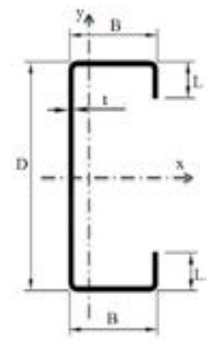

Figure 2. The nominal dimensions of the channel section

$$P_y = \frac{\pi^2 EI_y}{(K_y L_y)^2} \quad (6)$$

$$P_z = \left[\frac{\pi^2 EC_W}{(K_t L_t)^2} + GJ\right]\left(\frac{1}{r_o^2}\right) \quad (7)$$

The channel section considered in this paper is the single-symmetric section (strong axis), therefore, the shear centre coordinate y0 = 0 (see Figure 2), and formula (4) is converted into:

$$(P_{cre} - P_y)\left[r_o^2(P_{cre} - P_x)(P_{cre} - P_z) - (P_{cre})^2(x_o)^2\right] = 0 \quad (8)$$

The solutions of (8) include:

$$P_{cre} = P_y \quad (9)$$

$$P_{cre} = P_{xz} = \frac{(P_x + P_z) \pm \sqrt{(P_x + P_z)^2 - 4P_x P_z\left(r_0^2 - x_0^2\right)/r_0^2}}{2\left(r_0^2 - x_0^2\right)/r_0^2} \quad (10)$$

The channel column can be buckled due to the flexural buckling according to the y-axis or flexural-torsional buckling according to the x and z axes.

3. Experiment on the flexural-torsional buckling of cold-formed channel columns

The paper presents the experimental setup and buckling behavior of cold-formed aluminum channel columns, which is part of the aluminium project number LP140100563 funded by the Australian Government, conducted at the University of Sydney. The cross-sections were selected from the BlueScope Permalite manufacturer's catalog[9], with heights ranging from 100mm to 400mm and thicknesses

(a) The compression test rig

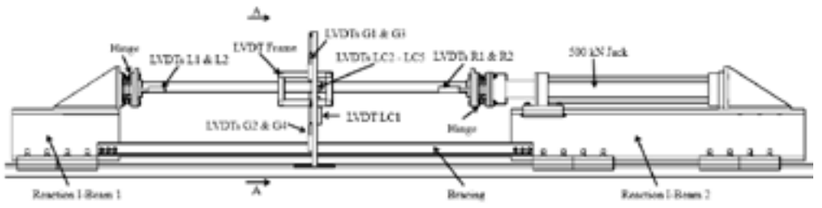

(b) Front view

Figure 3. Compression test set-up

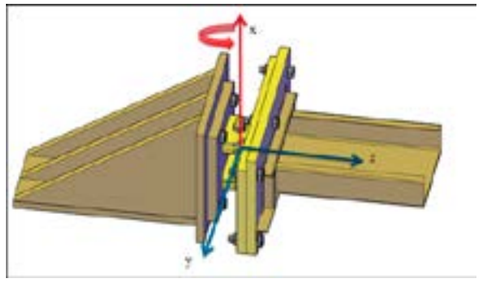

Figure 4. The end boundary condition of the test

Table 1. The test results for C10030 specimens

Specimens	Test results	Global buckling load (kN)
C10030-2.0m-1	91.25	96.10
C10030-2.0m-1e	81.00	
C10030-2.0m-2e	81.38	
C10030-2.5m-1	70.64	61.50
C10030-2.5m-2e	60.10	
C10030-2.5m-3e	61.60	
C10030-3.0m-2	49.45	44.30
C10030-3.0m-1e	46.76	
C10030-3.0m-3e	44.65	

Note: “e” stands for the eccentricity test.

of 2.5mm and 3mm. The specific cross-section chosen for analysis is C10030 (height 100mm and thickness 3mm) to observe global buckling without the influence of other buckling modes. The geometric dimensions of the C10030 section are as follows: D = 105mm; B = 59mm; L = 16mm; t = 3.0mm, where D, B, L and t are illustrated in Figure 2.

The specimens' lengths were chosen specifically to facilitate global buckling. The global buckling load is determined as the lower value between the flexural (Py) and flexural-torsional buckling loads (Pxz), calculated as presented in Section 2. To obtain the flexural-torsional buckling mode, the ends should be fixed in the y-axis and should be hinged in the x-axis.

The test rig, illustrated in Figure 3, featured two reaction I-beams securely clamped onto a rail system anchored into the strong floor. This configuration ensured the stability of the reaction I-beams during testing, preventing them from dislodging from the ground. To further secure the setup, two brace angle sections measuring L100mm×100mm×10mm were affixed through the web of each reaction I-beam using three M20 high-strength 8.8 bolts, effectively preventing any sliding of the reaction I-beams during testing. Despite

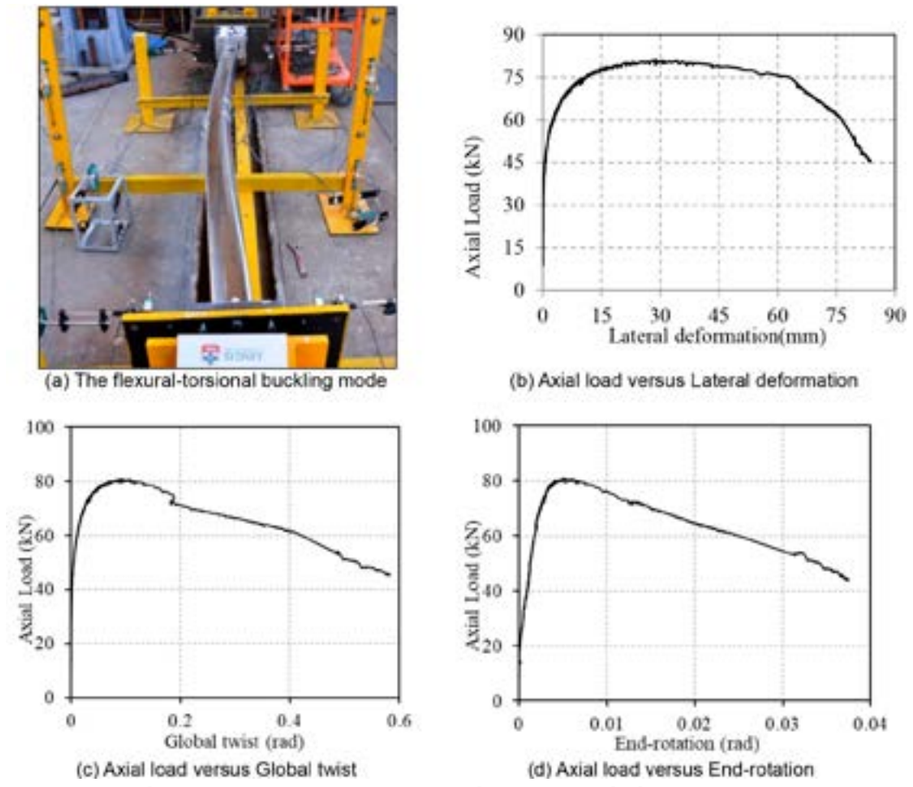

Figure 5. The test results of C10030-2.0m-1e in the first configuration [10]

the horizontal orientation of the specimens, the negligible self-weight of the aluminum alloy specimens was accounted for. A 500 kN MOOG jack was affixed atop reaction I-beam 2 to apply load to the specimens, as depicted in Figure 3.

In terms of end boundary conditions, the end sections of the specimens are allowed to rotate freely around the major axis, while their rotation is restricted in the minor axis (see Figure 4).The distances from the ends of the specimen to the center of the hinges are 75 mm each.

The displacements of the specimen were monitored using 13 transducers, as depicted in Figure 3. Four transducers, including LVDTs (L1, L2) on the left side and (R1, R2) on the right side, were attached at the specimen ends to measure end rotations and axial shortening. Additionally, five transducers from LC1 to LC5 were mounted on an aluminum transducer frame at two corners of the web and the flanges, as shown in Figure 2(c). This arrangement allowed the LVDTs on the transducer frame to measure local cross-section distortion at the mid-length during global buckling. To assess global deformations, four transducers labeled G1 to G4 were fixed to two stable columns and linked to the transducer frame's corners using four steel strings, as illustrated in Figure 2(c). By analyzing data from these transducers, including lateral deformation and global twist, the global deformations of the specimens were determined. The first step involved calculating the displacements of the transducer frame's two corners in the x and y directions. Subsequently, using the transducer frame's dimensions and the specimen's centroid, the displacements of the centroid and the specimen's global twist at the mid-length were computed.

The specimens underwent testing under both concentric and eccentric conditions. Concentric tests were conducted to verify the elastic buckling loads, while eccentric tests were carried out for design purposes with a nominal eccentricity of Le/1500 at both ends of each specimen, where Le represents the actual length of the specimen.

For the C10030 section across all examined lengths, the failure modes were observed in the flexural-torsional buckling mode, as depicted in Figure 5(a). The local buckling mode was not observed since the ultimate load is significantly lower than the local buckling load. Figures 5(b) and 5(c) show that the deformations of the specimen occurred simultaneously with both twist and lateral displacement, therefore, the lateral-torsional buckling mode was obtained in this experiment.

The test results of all C10030 specimens were collected and listed in Table 1. Also, the elastic buckling loads of test specimens were determined according to Section 2 with the Young modulus E = 70 GPa as presented in Pham et al [10]. In Table 1, it is found that the strengths of the concentric C10030-2.5m-1 and C10030-3.0m-2 specimensare slightly higher than their elastic global buckling loads. This phenomenon is attributed to the post-buckling behavior in torsion, as discussed and explained in Trahair's research[11].

4. Conclusions

The paper presented the theoretical principles for calculating the global buckling load of cold-formed structural columns, with a specific focus on applying these principles to determine the global buckling loads for the cold-formed channel column subject to flexural-torsional buckling. Subsequently, the paper summarized the experimental configuration and performance of a cold-formed aluminum column program to investigate the flexural-torsional buckling. The comparisons were carried out between theoretical predictions with experimental results to enhance understanding of the behavior of cold-formed channel columns. It was found that the strengths of columns undergoing flexural-torsional buckling can be higher than the elastic buckling loads due to the post-buckling behavior in torsion./.

References

1. *N. H. Pham and Q. A. Vu, “Effects of stiffeners on the capacities of cold-formed steel channel members,” Steel Construction, vol. 14, no. 4, pp. 270–278, 2021, doi: 10.1002/stco.202100003.*
2. *S. P. Timoshenko and M. G. James, Theory of Elastic Stability, 2nd edition. New York: McGraw-Hill., 1961.*
3. *W. W. Yu, Cold-Formed Steel Structures. Huntington, New York: Robert E. Krieger Publishing Company, 1979.*
4. *N.S. Trahair. Flexural-Torsional Buckling of Structures, E.&F.N.Spon, 1993.*
5. *A. Chajes, P.J. Fang, and G. Winter, Torsional-Flexural Buckling, Elastic and Inelastic of Cold-Formed Thin-Walled Columns. Engineering Research Bulletin 66-1, Cornell University, Ithaca, NY, 1966.*
6. *A. Chajes, and G. Winter, “Torsional-Flexural Buckling of Thin-Walled Members”, Journal of the Structural Division, vol. 91, 1965.*
7. *J. Becque, “The Interaction of Local and Overall Buckling of Cold-Formed Stainless Steel Columns,” University of Sydney: Sydney, Australia, 2008.*
8. *J. Becque and K. J. R. Rasmussen, “Experimental investigation of local-overall interaction buckling of stainless-steel lipped channel columns,” J Constr Steel Res, vol. 65, no. 8–9, pp. 1677–1684, 2009, doi: 10.1016/j.jcsr.2009.04.025.*
9. *Permalite - Aluminium Roll-formed Purlin Solutions, PermaliteAluminium Building Solutions Pty Ltd. Eagle Farm Qld 4009, Australia: Blue Scope Lysaghts, 2015.*
10. *N. H. Pham, C. H. Pham, and K. J. R. Rasmussen, “Experimental Investigation of The Member Buckling of Cold-rolled Aluminium Alloy 5052 Channel Columns,” in Proceeding of 9th International Conference on Advances in Steel Structures, Hong Kong, 2018. doi: 10.18057/ICASS2018.P.111.*
11. *N. S. Trahair, “Post-buckling strength of steel tee columns,” Journal of Engineering Structures, vol. 7, no. 56, pp. 1800–1807, 2013, doi: 10.1016/j.engstruct.2013.07.023.*